Investigation of the influence of an excavation on adjacent excavations, using neural networks

by S. Kwon and J.W. Wilson*

Synopsis

When an underground excavation is created near to an instrumented measuring location, deformation at the location increases. The characteristics of this deformation increase, as well as the duration of the influence caused by the adjacent excavation, is dependent on parameters such as opening geometry and measuring location. In this study, neural networks were applied to investigate the deformation increase and the influence of each parameter on the deformation change derived from extensometer measurements at the Waste Isolation Pilot Plant (WIPP) site in New Mexico, USA.

Introduction

The characteristics of the response of the rock mass around an opening to an adjacent or nearby excavation are important in designing optimum mining sequences, as well as an adequate mining method. Also, it is possible to estimate the elastic deformational behaviour immediately after creating an excavation by investigating the response of the rock mass to the sudden stress change due to this adjacent excavation. The effect of an adjacent excavation on an existing excavation can be clearly shown by various types of displacement plots. When an excavation is created near the measuring location, the deformation of the location increases rapidly as the adjacent excavation is created. The amount of deformation increase caused by adjacent mining seems to be dependent on several factors such as the mining method, the measuring location, the distance between the measuring location and the newly excavated opening, and opening geometry. The duration of influence can also be affected by these factors. Thus, the prediction of the influence of an adjacent excavation on the deformation and deformation rate change, is especially difficult.

The application of neural networks can provide a useful tool for predicting the influence of an adjacent excavation on existing mine workings, and for deriving relationships between deformation change due to the adjacent excavation and each parameter. This is possible because of the following reasons: firstly, neural networks can use qualitative information as input or output. Regression equations require only quantitative information for input, but in neural networks, qualitative parameters such as rock type, location of measurement, or mining type can also be incorporated; secondly, there is no limit to the number of inputs or outputs; thirdly, neural networks can be used to solve complicated non-linear problems, and complex relationships between input and output; and finally, it is not necessary to know the general relationship between input and output variables before carrying out the data analysis. Neural networks are capable of modelling input-output functional relations, even when mathematically explicit formulas are unavailable (Szewczyk and Hajela, 1994).

Brief introduction to the waste isolation pilot plant

The WIPP is a research and development facility authorized to demonstrate the safe disposal of transuranic radioactive waste arising from United States defence programmes. The WIPP project began construction of a facility in Carlsbad, New Mexico under the direction of U.S. Department of Energy (DOE) in 1981. The underground facility at the WIPP is located 650 m below surface in 900 m thick bedded rock salt deposits formed approximately 225 million years ago. Rock salt formations have been recommended as one of the leading candidates for the permanent disposal of radioactive nuclear wastes. The principal advantages of salt include:

- salt deposits are found in stable geological areas with very little earthquake activity

* *Department of Mining Engineering, University of Missouri-Rolla.*

 SA ISSN 0038–223X/3.00 + 0.00. Paper received Jan. 1998; revised paper received May 1998.

- salt deposits demonstrate the absence of flowing fresh water, because water would have dissolved the salt beds
- salt is relatively easy to mine
- salt has the ability to heal fractures because of its plastic quality, i.e. creep with time.

The WIPP facility is composed of surface buildings, vertical shafts, and a series of horizontal underground storage rooms, alcoves, and tunnels. The underground site has been divided into three areas (Munson *et al.*, 1990):

- the Site and Preliminary Design Validation (SPDV) area
- the Experimental area
- the TRU waste storage area.

The SPDV area, the experimental area, and Panel 1 in the storage area have been completed and data are being collected from various measuring instruments. The storage area will be made up of eight panels consisting of seven rooms each where each room is approximately 4 m high, 10 m wide and 100 m long. The four rooms in the SPDV area have similar configurations to the rooms in the waste storage area and all of the underground openings are rectangular in cross-section. The drift configuration ranges from 2.4 m to 3.6 m high and 3.6 m to 7.6 m wide. Figure 1 shows a schematic drawing of the underground facilities at the WIPP.

Introduction to neural networks

The human brain is a very complex biological network of hundreds of billions of special cells called neurons and connections between neurons, called dendrites. Figure 2 shows the major components of a typical biological nerve cell. Each neuron is connected to 1,000 or more other neurons through its branching mesh. These neurons transmit an electrical impulse received from neighbouring neurons through a channel, called an axon, to other connected neurons. When the pulse reaches the end of the axon, it must cross a gap about a millionth of an inch wide, called a synapse, in order to reach the neighbouring neurons. When the electrical signal stimulates the axon, a chemical substance referred to as a 'neurotransmitter' will be released. The neurotransmitter moves to the dendrites of the receiving neuron and generates an electrical impulse. Depending on the chemical substance generated, different electrical signals can be formed in the synapse; either excitatory (decreasing the polarization of the cell) or inhibitory (increasing the polarization of the cell). The different electrical input signals from the numerous neighbouring neurons are summed at the axon hillock. When the amount of depolarization stored at the axon hillock is sufficient, an action potential is generated and travels down the axon away from the main cell body. In this manner, a conversion occurs between an electrical signal and a chemical signal, and a message can be continuously transmitted from one neuron to another until the impulse no longer exceeds the threshold at the axon hillock. There are a few theories about how the brain can learn, but the general opinion is that learning in the brain occurs in the form of changes in the synapses when signals are received (Lawrence, 1993).

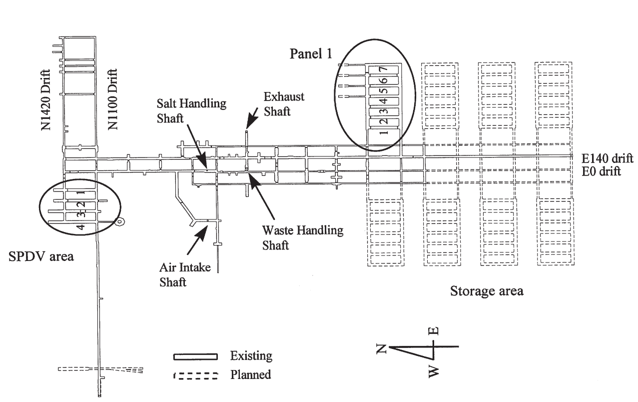

Figure 1—Underground layout of the WIPP facility

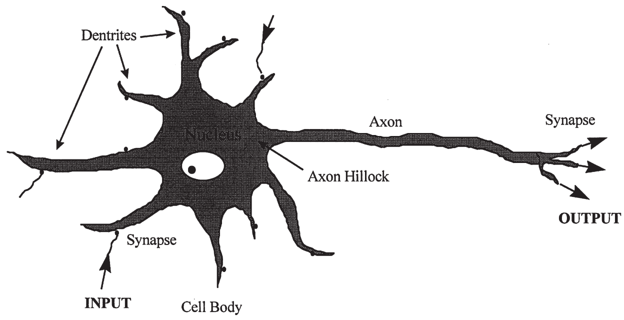

Figure 2—Typical biological neuron

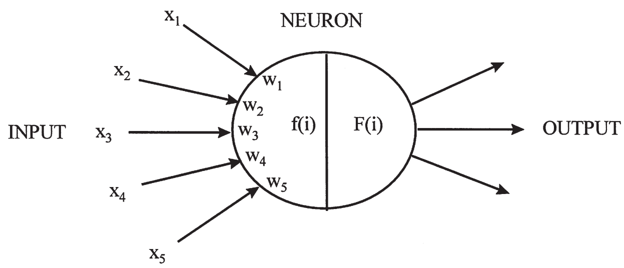

$$f(i) = w_1x_1 + w_2x_2 + w_3x_3 + w_4x_4 + w_5x_5$$
$$F(i) = \text{Transformation of } f(i)$$

Figure 3—Artificial neuron

Neural networks, specifically artificial neural networks, were developed to mathematically simulate the mechanism of a human brain in learning. Artificial neural networks are formed of simulated neurons, connected in a similar way to the neurons in a human brain and thus are able to learn in a similar manner as the human brain, as shown in Figure 3.

The basic process in neural networks can be divided into four steps;

- input to the neurons
- summation of the net values calculated by multiplying the weight values and input values of the individual input signals
- transformation of the net value
- output to the next neuron.

Input in neural networks simulates the electrical signal coming from the synapses. Calculation of the net value simulates the summation of the potential delivered from the neighbouring neurons at the axon hillock. The weights in neural networks serve a similar function to the neurotransmitter in the synapse, because it is the weight in the neural network which determines whether the input signal is excitatory or inhibitory. Transformation of the net value is required to simulate the function of the axon hillock which determines whether the signal can be transmitted to the next neuron or not. Similar to the human brain, neural networks are highly parallel dynamic systems that transfer information by means of their overall state response to input. Sometimes this is called an artificial neural system, neural intelligence, or neurocomputer. After the initial neural network model was developed in 1943, many other techniques including Back-propagation (BP) were developed. Each technique has its own characteristics and can be applied to different areas, mainly for noise reduction, pattern recognition, performance prediction, and performance optimization.

Recently, neural networks were applied to rock mechanics and rock engineering. Zhang *et al.*, (1991) applied neural networks to analyze the relationship between the physical properties of rock samples and their elastic linear compressibility. Neural network techniques have since been applied to identify probable failure modes for underground openings from prior case history information (Sterling and Lee,1992; and Lee and Sterling, 1992), to characterize the main elements in longwall chain pillar design (Zhang, 1995), and to determine the relationship between geological variables and possible fracture conditions (Thomas and La Pointe, 1995). In a study described in this paper, a three-layer back-propagation network was developed to investigate the influence of an adjacent excavation on the deformation measurements in an existing mine opening and also the relationships between the influence and each parameter.

Back-propagation

Back-propagation (BP) is a multi-layer feed-forward network that uses a supervised learning method in which an error signal is fed back through the network and changes network values to correct the error and to prevent the same error from happening again (Lawrence, 1993). It is the most commonly used neural network model because it provides a mathematical explanation for the dynamics of learning and has proved to be consistent and reliable when applied (Lawrence, 1993). BP is suitable for predicting opening deformations, since most of the input and output values are analog. Many of other neural network models which require binary or bipolar information, are not suitable for predicting the relationship between analog input and output.

Structure of the back-propagation network

In BP, three-layer and four-layer networks are most popular. The three-layer network consists of three layers: input, hidden, and output layers. The three-layer BP architecture is shown in Figure 4. The input layer neurons send information to the hidden layer neurons between the input and output layers. The number of neurons in each layer depends on the number of input and output parameters. There is no formula to determine how many hidden neurons are best for the network, because it seems to be largely dependent upon the complexity of the problem being solved (Lawrence, 1993).

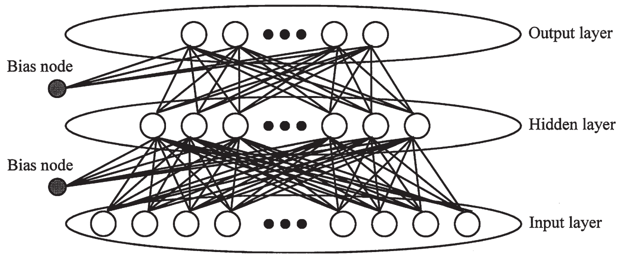

Figure 4—Architecture of three-layer back-propagation

One rule of thumb is to use the average of the number of inputs and the number of output neurons (Lawrence, 1993).

Each connection has a weight which can represent the strength of the relationship between connected nodes. During network training, the weights of the connections are changed to minimize the overall error term. The error of the network is determined by comparing the desired output and calculated output. In neural networks, changing the weights is called learning. Bias terms can be included to help to obtain convergence of the weights to an acceptable solution (Freeman and Skapura, 1992).

Activation function

The activation function is applied to the net input of a neuron and determines the output from the neuron. Its domain must be all real numbers, as there is no theoretical limit to the net input (Master, 1993). The range of the activation function is usually limited and usually ranges between 0 and 1, but some range from -1 to 1. Early neural models used a simple threshold function as follows:

$$f(x) = \begin{cases} 1, x \geq \delta \\ 0, x < \delta \end{cases} \qquad [1]$$

where, δ is the threshold value. If the weighted sum of inputs is less than the threshold, the neuron's output is 0, otherwise the output is 1. In some models the output would be the weighted sum itself, if the threshold value were exceeded (Master, 1993).

There are great advantages to the activation function, being differentiable in describing the learning mechanism of the network mathematically. Since the threshold function is not differentiable, many neural network models, including BP, use a sigmoid activation function, which is differentiable but otherwise acts in a similar way to the threshold function. Figure 5 shows the characteristic S-shape of the sigmoid function and typical threshold function. The typical sigmoid function is

$$f(x) = \frac{1}{1 + e^{\pm x}} \qquad [2]$$

A sigmoid function is a non-linear but continuous, real-valued function whose domain is real, whose derivative is always positive, and whose range is bounded. In most cases, it has been found that the exact shape of the function has little effect on the ultimate power of the network, though it can have a significant impact on the training speed.

Generalized delta rule

BP network uses a generalized delta rule as the learning algorithm. The learning rule is the most important part of a neural network, since it determines how the weights are adjusted as the neural network gains experience (Lawrence, 1993). For a single output unit k, the error is the difference between the desired output value Y_k and the calculated output O_k.

$$\Delta_k = Y_k \pm O_k \qquad [3]$$

During a program run, the sum of the squares of the errors for all output units should be minimized.

$$E = \frac{1}{2}\sum_{k=1}^{m} \Delta_k^{\,2} \qquad [4]$$

With the generalized delta rule, the network can reduce the sum of the squared error at each iteration step, by changing the weights applied to all the connections.

Calculation procedure

The calculation process for BP is as follows:

a. Initialize weight values w_{ij} using a random number generating function for each weight.
b. Apply the input vector, $X=(x_1,x_2,....,x_n)^T$ to the input units.
c. Calculate the net-input feed to the hidden layer nodes by multiplying the weight and input values for each input node.
d. Add a bias term to each input feed using the following equation. The bias term is usually added to accelerate convergence of the weight values to an acceptable solution.

$$net_j^{\,h} = \sum_{i=1}^{n} w_{ji}^{\,h} x_i + \theta_j^{\,h} \qquad [5]$$

NOTE: *net* is representing the net value of a node. The net value is calculated by summing the input value multiplied by their corresponding weights and bias value of the hidden layer, as shown in Equation 5. '*net jh*' in Equation 5 is the net value of a node in the hidden layer. In this operation, the subscripts represent each connected node and each superscript represents a layer. For example, $w_{ji}h$ is the weight applied to the connection between node i of the input layer and node j of the hidden layer. θ_j^h is the bias term for node j of the hidden layer.

e. Calculate the outputs from the hidden layer using an activation function f for the number of the hidden layer:

$$I_j = f_j^{\,h}\left(net_j^{\,h}\right) \qquad [6]$$

f. Move to the output layer and calculate the net-input values for each unit from the hidden layer nodes connected to it

$$net_k^{\,O} = \sum_{j=1}^{m} w_{kj}^{\,O} I_j + \theta_k^{\,O} \qquad [7]$$

g. Calculate the output from the output layers.

$$O_k = f_k^{\,O}\left(net_k^{\,O}\right) \qquad [8]$$

h. Calculate the error term for the current output values. Based on the generalized delta rule, the error term of the output layer can be determined.

$$\Delta_k^{\,O} = \left(Y_k \pm O_k\right) f_k^{\,O'}\left(net_k^{\,O}\right) \qquad [9]$$

where, Y_k is the desired output value and $f_{kO'}$ is the derivative of the activation function.

i. Upgrade weights on the output layer by using the calculated error term.

$$w_{kj}^{\,O}(t+1) = w_{kj}^{\,O}(t) + \eta \Delta_k^{\,O} I_j \qquad [10]$$

NOTE: 't' represents t'th iteration.
where, η is the learning rate which can control the learning speed. The learning rate determines the size of weight adjustment in the network when there is error in the network, i.e. difference between the known output and calculated output. Selection of a value for the learning rate parameter has a significant effect on the network performance. Usually, η needs to be a small number in the order of 0.05 to 0.25 to ensure that the network converges to a solution (Freeman and Skapura, 1992). With a small value of η, the network is trained with a large number of iterations, while a large η may bounce the network around too far from the actual solution. It is recommended to use a small learning rate initially and increase it as the network error decreases.

j. Calculate the error term for the hidden layer.

$$\Delta_j^{\,h} = f_j^{\,h'}\left(net_j^{\,h}\right) \sum_{k=1}^{l} \Delta_k^{\,O} w_{kj}^{\,O} \qquad [11]$$

NOTE: Net$j$, h in Equations [6] and [11] represents the net value of a node, j, of the hidden layer, h, and calculated from Equation [5]. Net k, o in Equation [9] represents the net value of a node, k, of the output layer, o, and calculated from Equation 7.

k. Update weights used in the hidden layer.

$$w_{ji}^{\,h}(t+1) = w_{ji}^{\,h}(t) + \eta \Delta_j^{\,h} x_i \qquad [12]$$

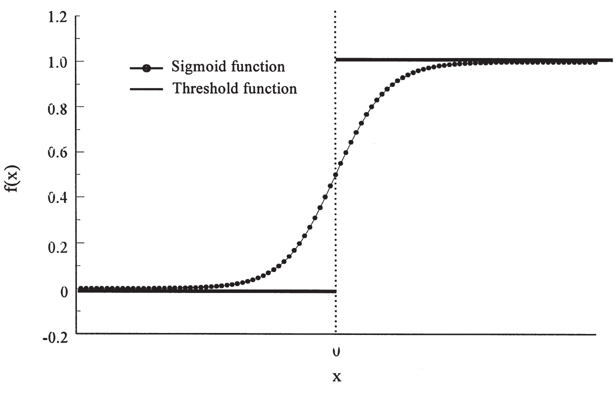

Figure 5—Typical activation functions

Influence of an adjacent excavation to an existing excavation

Figure 6 and Figure 7 show how the typical curves of deformation and deformation rate vary at an existing excavation under the influence of an adjacent excavation.

The mining of the adjacent excavation causes an immediate increase in the deformation and deformation rate of the existing excavations. Since the excavation of the adjacent mining takes time, there is an offset of the peak value from the date of the creation of the adjacent excavation. The deformation rate then decays exponentially from the peak value back to the rate that the existing excavation was experiencing before the adjacent mining took place. A similar deformation increase can be detected if the opening geometry is changed, such as by floor trimming.

The abrupt increase in the opening deformation may affect the overall stability of an opening. In this study, therefore, several parameters for determining the effect of adjacent mining were considered and were calculated using the extension measurements at WIPP. From the calculations, the influence of controlling factors on the deformation change caused by the excavation of an adjacent opening, was investigated.

Cases showing the influence of adjacent mining

The influence of adjacent excavations was observed in the measurements from the WIPP site and at several other mines.

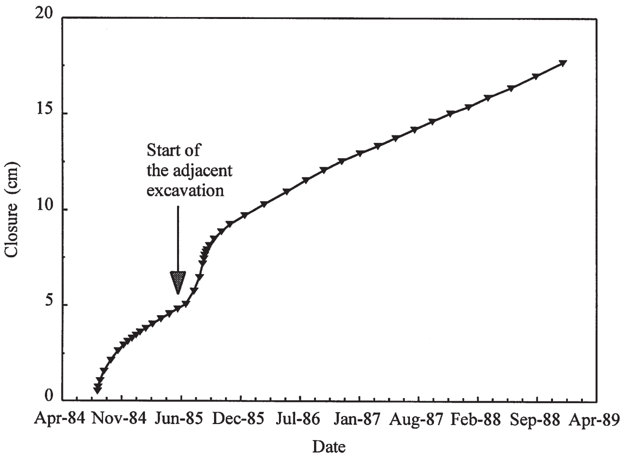

Figure 6—Sudden closure increase due to the creation of an adjacent excavation

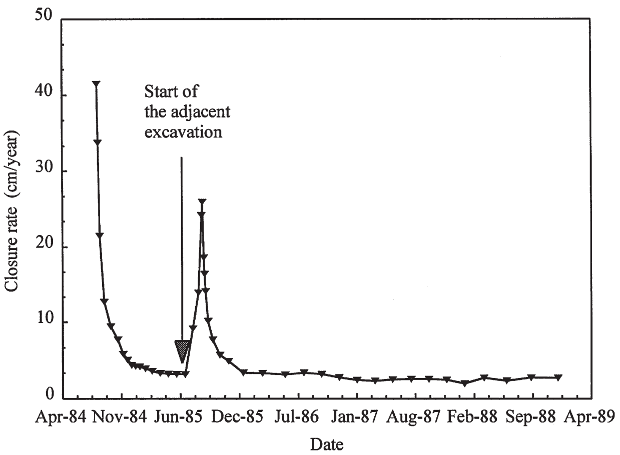

Figure 7—Typical pattern of closure rate change after the creation of an adjacent excavation

The following cases are outstanding examples showing the significant influence of new adjacent excavations on existing mine openings.

Panel 1 at WIPP

The seven rooms in the Panel 1 area at WIPP were excavated in 1986 for emplacing nuclear waste material. Figure 8 shows the layout of the Panel 1 area. The alcoves, TA1, TA2, TA3, and TA4, were excavated from June 1989 to July 1989. The roof conditions of Rooms 4, 5, 6, and 7 are less stable than Rooms 1, 2, and 3 from observation reports. This could be related to the excavation of the alcoves, as well as the excavation sequence of the rooms themselves. Figure 9 shows the closure rate contours in the Panel 1 area before and after the excavation of the alcoves. The closure rates near the alcoves increased significantly after the excavation, and several months after the excavation of these alcoves the closure rates decayed back to the closure rate before the excavation took place.

SPDV rooms at WIPP

In the Site and Preliminary Design Validation (SPDV) area, four rooms had been excavated in the following excavation sequence: Room 2 (Mar. 10, 1983), Room 3 (Mar. 25, 1983), Room 1 (Apr. 4, 1983), and Room 4 (Apr. 20, 1983). Figure 10 shows the excavation sequence and the dimensions in the SPDV area. Because of the time interval between each excavation, the deformation of pre-excavated rooms was influenced by the subsequent excavations. Figure 11 illustrates the influence of subsequent excavations on the rib deformation 1–7.6 m of pre-excavated rooms. Even though the pillar between each opening is 100 feet wide, the effect of subsequent excavations is clearly shown in the bay strain rate plots. The most dramatic change was on the rate curve of the East rib of Room 2 when Room 1 was mined. The bay strain in the Room 2 East rib increased about 100% from 0.076 cm/year to 0.15 cm/year. The effect of the adjacent excavations appeared on the strain rate curves almost immediately, and this implies that the stress redistribution due to the additional excavations developed very rapidly. The influence of adjacent mining has shown a similar effect in deeper rock, that is, beyond 7.6 m from the opening (Kwon, 1996).

Calculation of the influence of an adjacent excavation on a nearby existing excavation

Several parameters can be used to measure the influence of adjacent mining on existing rooms. In this study

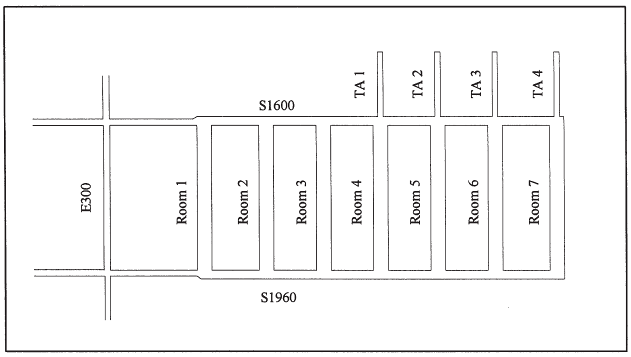

Figure 8—Plan view of the Panel 1 area

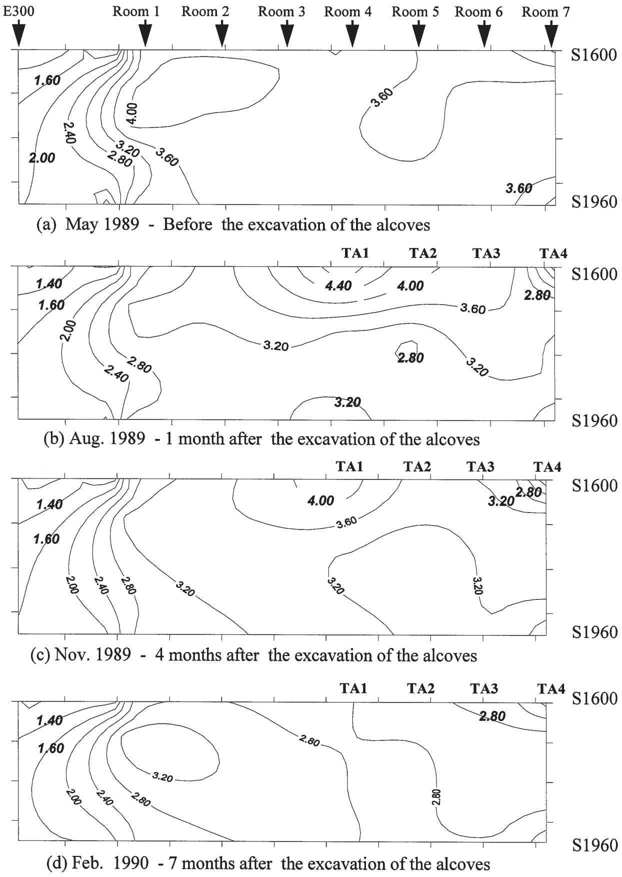

Figure 9—Closure rate contours (cm/year) in the Panel 1 area

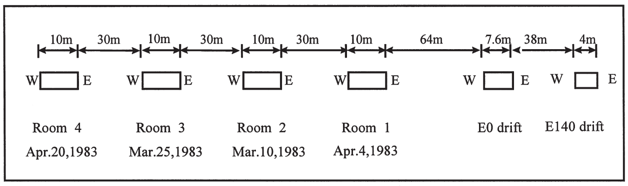

Figure 10—Dimensions and excavation dates of the openings in the SPDV area

- ➤ peak extension rate
- ➤ duration of influence, and
- ➤ area increase for a specific time period on displacement or displacement rate plots, were suggested as the parameters. Figure 12 and Figure 13 show how to determine these parameters. The peak extension rate after the adjacent excavation was not included in this study, because of its sensitivity to the measuring interval compared to the other parameters (Kwon, 1996).

The increased movement caused by an adjacent excavation was separated from the original extension measurements and a curve fitted to find the best equation to describe the effect of time, and then extension rates were calculated from the curve fitting equation. Next, the suggested parameters were calculated from the extension and extension rate curves. The parameters which characterize the influence of adjacent mining or floor trimming on different

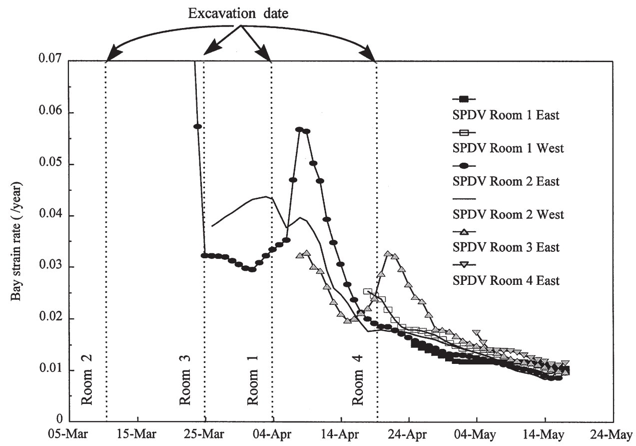

Figure 11—Strain rate change in the ribs (1 - 7.6 m) due to adjacent excavations in the SPDV area

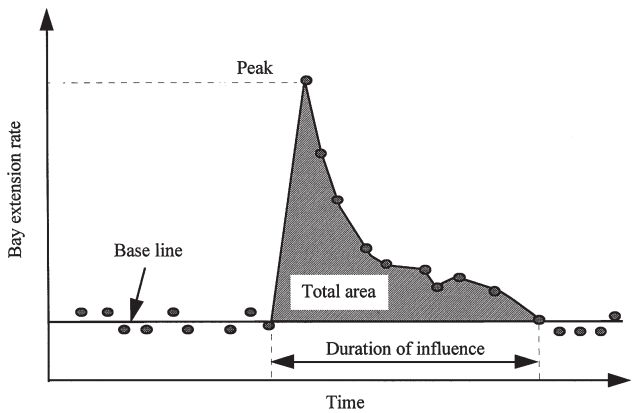

Figure 12—Parameters to evaluate the influence of an adjacent excavation

measuring locations, are listed in Table I. All listed extensometers have the same measuring range, namely 1–15 m. Mining type, elapsed days since excavation and before adjacent mining, measurement location, and opening geometry of each case, are listed together to check the relationship between each factor and the amount of extension increase due to the creation of adjacent excavations. Mining types or procedures, are illustrated in Figure 14.

Prediction of the influence of adjacent excavation using neural network

Selection of important parameters

To predict the influence of an adjacent excavation, the important parameters were identified. Based on previous data analyses, the following 9 parameters were chosen as the input for the network.

- ➤ Location of the measuring instrument: Since the influence of an adjacent excavation on the deformation change might be different when the measuring instrument is located in the roof , rib, or floor, the location of the instrument was included as an input parameter.

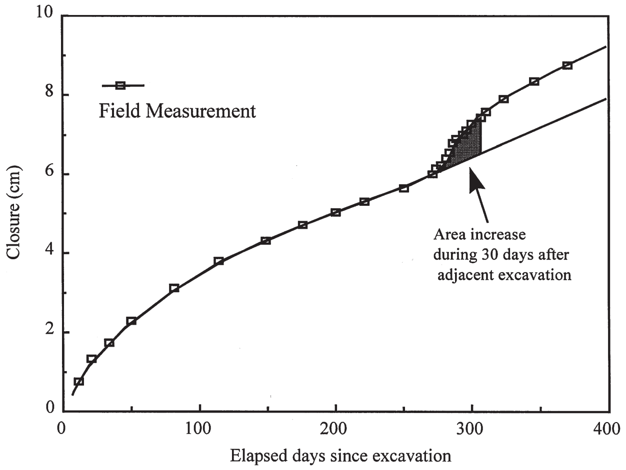

Figure 13—Description of the area increase during 30 days after the creation of an adjacent excavation

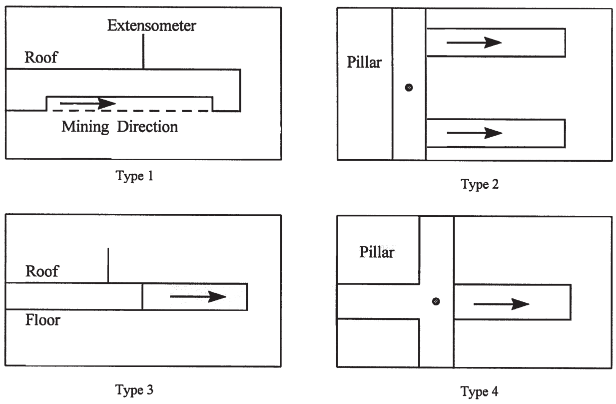

Figure 14—Four different types of mining an adjacent excavation

- Opening height: Opening height should be included, since it determines the width-to-height ratio of the pillars which can control the deformational behaviour.
- Opening width: Opening width is an important parameter on control of the vertical deformation of the excavation, since it determines the length of the roof beam, and thus the structural integrity of the opening.
- Maximum and minimum pillar sizes around the opening. The size of the pillar around an excavation can determine the overall extraction ratio and thus the stress concentration in the pillar.
- Base extension rate: The extension rate immediately before the adjacent excavation might determine the overall influence of the adjacent excavation.
- Mining type: Mining types as shown in Figure 14 were included as an input parameter.
- Elapsed days since initial excavation until the adjacent excavation: Depending on the creep stage, the influence of the adjacent excavation could be different.
- Time after the adjacent excavation: Since rock salt deforms time-dependently, time should be included as an important parameter for predicting the deformation change.

Back-propagation structure

A three-layer back-propagation network was used to predict the influence of newly mined adjacent excavations on the deformation measurements in existing mine openings. The three layers consist of 9 input nodes for the 9 input parameters, 4 hidden nodes, and 1 output node for extension. Bias terms for the hidden and output layers were included to help the convergence of the weights to an acceptable solution. The bias terms act as an extra degree of freedom, and its use is largely a matter of experimentation with the specific application. The initial weight of connection was set up using a random number generating function. The

Table I

Influence of adjacent excavation on an existing room using different parameters

Location H (ft) x W (ft)	Elapsed days since excavation	Mining Type	30 days extension area (cm.day)	Overall extention increase (cm)	Extension increase over 30 days (cm)	Duration of mining influence (days)
Floor 12x20	399	type 4	10.69	1.16	0.5	230
Floor 13x33	414	type 4	17.53	1.25	0.8	200
Rib 12x25	278	type 1	8.02	0.74	0.49	125
Rib 8x14	317	type 2	1.5	0.17	0.1	163
Rib 8x14	317	type 2	2.61	0.27	0.13	141
Rib 12x25	278	type 1	8.11	0.69	0.48	125
Roof 12x14	685	type 4	10.78	0.58	0.47	179
Roof 12x20	399	type 4	23.97	2.04	1.03	223
Roof 12x25	330	type 1	9.83	0.61	0.38	85
Roof 12x25	537	type 4	29.11	2.81	1.34	345
Roof 12x25	959	type 4	9.58	1.03	0.58	126
Roof 12x25	1053	type 4	19.45	3.24	0.99	377
Roof 12x25	342	type 4	11.11	0.74	0.5	158
Roof 12x25	521	-	4.53	2.48	0.4	240
Roof 12x25	342	type 4	14.19	0.94	0.64	166
Roof 12x25	521	-	4.87	2.32	0.41	239
Roof 13x33	414	type 4	38.28	2.92	1.77	400
Roof 13x33	417	type 4	38.51	1.95	1.73	190
Roof 18x33	159	type 3	21.73	1.23	1.22	51
Roof 8x14	317	type 2	0.9	0.18	0.06	192

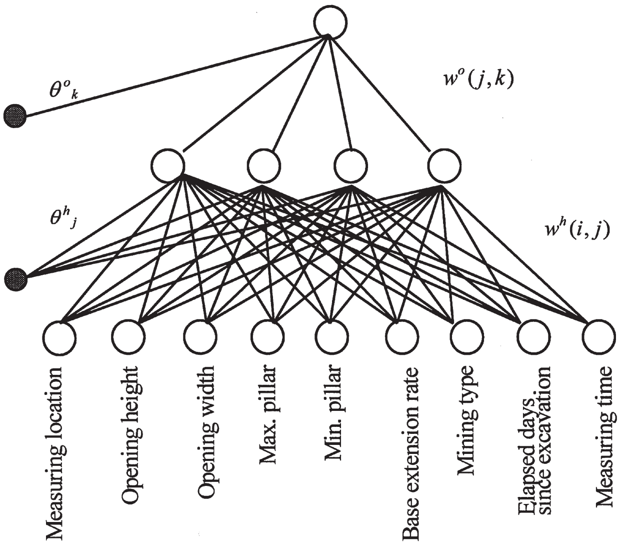

Figure 15—Back-propagation architecture for predicting the deformation change

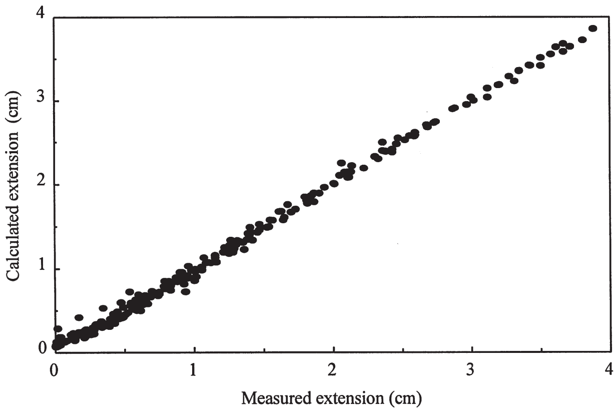

Figure 16—Extension prediction from the trained neural network

architecture of the back-propagation network used in this study is shown in Figure 15.

Data collection and training

The output in the neural network is the total extension measured from the extensometers. The extensometers installed at the WIPP site measure the extension between the opening surface and 15 m from the opening. The extension increase due to an adjacent excavation was fitted using power law equation, which was proved to be the best fitting equation, and the extension at different times was determined from the fitting curve for each case. The extension measurements listed in Table I were used for training the neural network. In order to train the network, 225 data points were selected from the extensometers. The inputs and outputs were normalized to lie in the range from 0 to 1. Normalization of data was carried out so that the range of values at each input and/or each output provided a better balance in the rate of learning in the network with respect to each independent and dependent variable (Flood and Kartam, 1994). When any value was infinite, it had to be defined by some large number. For example, width of an abutment pillar

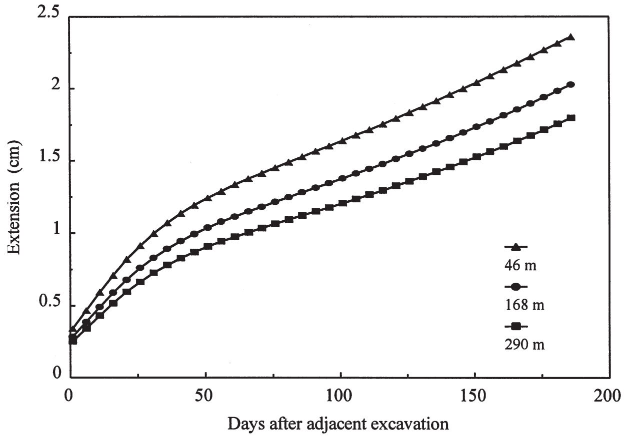

Figure 17—Influence of pillar size

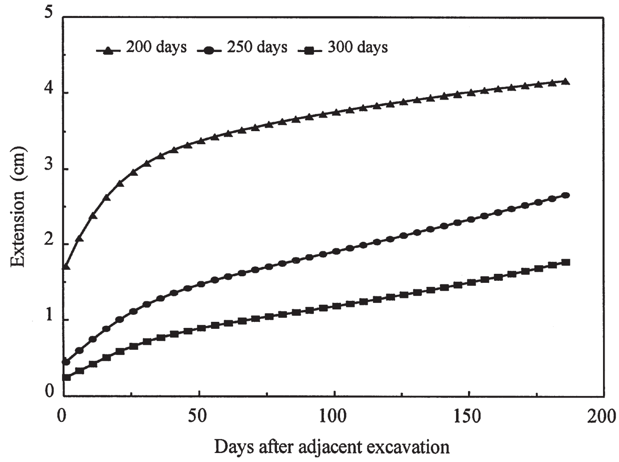

Figure 18—Influence of time interval between the excavation date of the measuring location and the new adjacent opening

was determined as 300 m. The normalized data were used to train the back-propagation network. Training was stopped when the variation in the error term of the network was negligible compared to the error term. Figure 16 shows a comparison between the measured and calculated extension increase due to an adjacent excavation, after training.

Training results

Using the trained network, it was possible to evaluate the influence of each parameter on the opening deformation. Figure 17 shows the influence of maximum pillar size around a measuring location on the extension change due to an adjacent excavation. In order to investigate the influence of each parameter, the roof extension was calculated from the trained neural network with different pillar sizes, while the other parameters are the same. With the increase of the maximum pillar size around the measuring location, the influence of the adjacent excavation on the deformation measurement decreases continuously. The predicted extension change due to an adjacent excavation from the Neural Network shows the same pattern as the typical creep curve, i.e. rapid deformation change in the early stages and then almost a constant deformation rate during the steady creep stage.

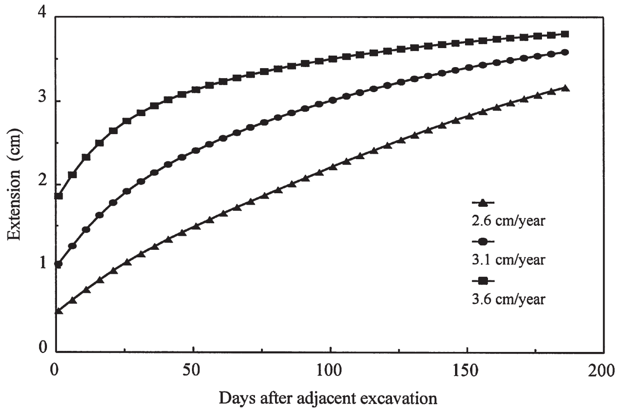

Figure 19—Influence of base extension rate before the mining of the adjacent excavation

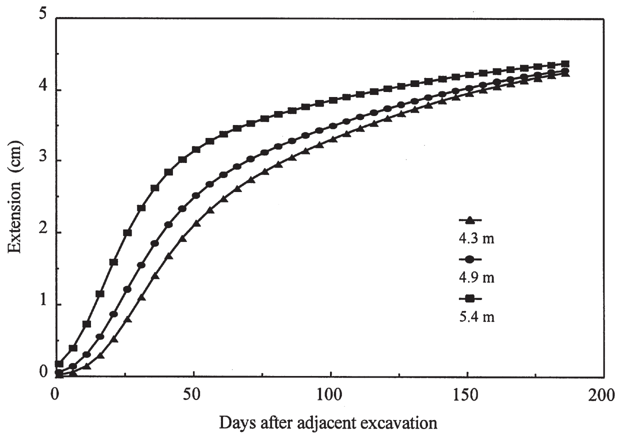

Figure 20—Influence of opening width

Depending on the time interval between the excavation date of the measuring location and the adjacent excavation, the roof extension increase due to the adjacent excavation shows different patterns. The influence of the excavation date of the adjacent excavation can be clearly shown in Figure 18. With a shorter time interval between the excavations, the extension change due to the adjacent excavation was more rapid and larger. From this result, it could be concluded that it is recommended to delay the mining of the adjacent excavation so as to decrease the extension change caused by the adjacent excavation. A similar conclusion can be drawn from Figure 19 which shows the influence of the base extension rate which is the extension rate immediately before mining of the the adjacent excavation. From Figure 19, the extension increase due to an adjacent excavation increases with base extension rate. Since the creep rate decreases almost exponentially in the primary creep stages, it would be possible to reduce the influence of the adjacent excavation on the deformation change at previously excavated openings by delaying the mining of the adjacent excavation. Another important issue in Figure 19 is that the extension increase immediately after the adjacent excavation was created, was predicted to increase with higher deformation rates immediately before the adjacent excavation. When the base deformation rate was 3.6 cm/year, the elastic deformation was as high as 2 cm.

Figure 20 and Figure 21 show the influence of opening width and opening height on the deformation increase caused by the mining of an adjacent excavation. With the increase of the opening width and height, additional extension increase was predicted. The significant influence of opening height was observable in Figure 21. With the increase of about 0.3 m increase in the opening height from 3.7 m to 4.0 m and from 4.0 m to 4.3 m, the extension increase due to the adjacent excavation changed significantly.

Advantages/disadvantages of the neural network approach as compared with conventional viscoplastic modelling

Computer simulations are currently the most popular method to describe the deformational behaviour of a rock mass around an excavation. If we use computer simulation, the stress and strain distribution around the excavation can be determined and this helps to explain the deformation mechanism around the excavation. Even though computer simulation techniques have many advantages, there are clear limitations to their use. Firstly, the *in situ* physical and mechanical properties of the rock should be precisely known in order to produce reliable results from computer simulation. Secondly, the changes in the mechanical and physical properties of the rocks after excavation should be mathematically expressed in constitutive equations in the computer simulation. Thirdly, the values for the parameters in the constitutive equations are usually obtained from laboratory tests and thus it is nearly impossible to predict accurately the actual complex deformational behaviour of rock salt. Therefore, the description of deformational behaviour of an underground excavation derived from a computer simulation can only be considered as a reference. In contrast, neural network does not require the physical mechanical properties of the rock, because the neural network uses *in situ* deformation measurements, which already include the effect of the parameters important to the deformational behaviour of underground excavations. Also, neural network can be applied to solve very complex nonlinear problems. Because of

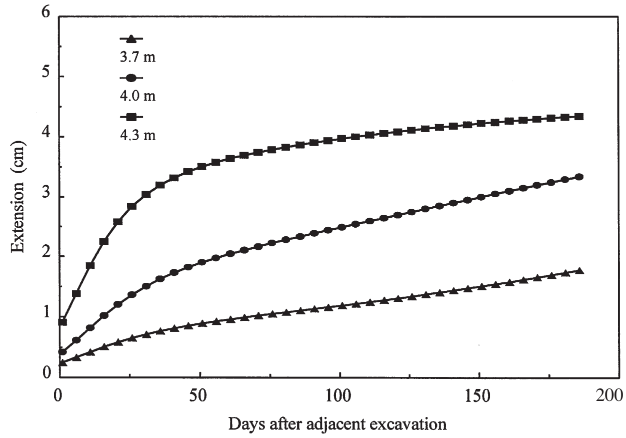

Figure 21—Influence of opening height

this, neural network can predict the deformation of an underground excavation more accurately than computer simulation if there is enough information.

The disadvantage of neural network analysis compared to computer simulation is that the neural network can only be used for the prediction of the trained properties. Because of this, neural network for predicting the deformation of underground excavations cannot predict the stress change. Therefore, it is not easy to explain the general deformation mechanism of an underground excavation.

Conclusions

The influence of an adjacent excavation on the deformational behaviour of previously excavated openings was investigated by using actual deformation measurements from the WIPP underground site and the application of a neural network. From this study, the following conclusions can be drawn.

- Floor extensions are usually less sensitive to adjacent excavations than roof and rib extensions. This may be related to the lesser deformations in the floor compared to the roof and rib.
- Duration of the influence depends upon the elapsed days before the adjacent mining occurs. When new adjacent excavation is started before the existing opening reaches the steady state creep stage, the duration of mining influence is significantly shorter than otherwise noted. Figure 7 shows the rapid disappearance of this effect. In the case of the SPDV Room 2, the influence of the Room 1 excavation lasted only about 10 days, while the duration of influence is usually longer than 100 days when the adjacent opening is excavated in the steady state creep stage.
- The overall extension increase caused by an adjacent excavation, that is, represented by the area below the extension rate curve, varies within a range of from 0.17 to 3.24 inches. This overall extension increase is important in characterizing the influence of the creation of an adjacent excavation, since it includes the sudden extension change as well as the duration of influence.
- The extension increase of over 30 days following the creation of an adjacent excavation, is a useful parameter for comparing the cases studied, because it is less dependent on the duration of the mining influence and most of the extension occurs during the first 30 days after the adjacent mining takes place. In many cases, the extension increase during this time is more than 70% of the extension increase.
- The mining pattern type 2 has less influence than the other mining types studied in this work. The differences between type 1, type 3, and type 4 are not clear at this stage.
- With the application of neural networks on the deformation measurements from excavations in a mine, it was possible to predict more accurately the overall influence of a newly created adjacent excavation on the deformational behaviour of the previously excavated openings. Furthermore, the effect of the parameters could be studied from the deformation prediction by using the neural network.
- From the neural network application, it was found that the time interval between the rooms in a mine is an important parameter which determines the influence of the adjacent excavation on the deformational behaviour of the previously excavated openings. As shown in Figure 18, the deformation change due to an adjacent excavation decreases with increase in time interval.

The deformation change following the excavation of a new adjacent opening is the reaction of the rock mass around an opening to the rapid stress change in the pillars created by the new excavations. This situation is similar to the deformational behaviour that occurs immediately after creating an excavation. Thus, if the deformation change is measured carefully as new adjacent mining takes place, it will aid in understanding the deformational behaviour before the installation of the measuring instruments. For example, both elastic and plastic components of the excavation effect can be identified, since the instrument is already in place; normally the measurement of the elastic component is lost since it occurs as the excavation is made and before the instruments can be installed.

The deformation caused by the creation of an adjacent excavation can be effectively used to assess these results by using a computer simulation. A comparison between the measured deformation after mining of an adjacent excavation and the prediction from a computer simulation can determine the reliability of the assumptions used, including rock properties, when used in applying the simulation model.

References

FLOOD, I. and KARTAM, N. Neural networks in civil engineering. I. Principles and understanding. *J. of Computing in Civil Eng.* 8, 1994. pp.131–148.

FREEMAN, J.A. and SKAPURA, D.M. Neural networks. Addison-Wesley Pub. Co., Massachussetts. 1992.

KWON, S. An investigation of the deformation of underground excavations in salt and potash mines, Ph.D. thesis, University of Missouri-Rolla. 1996.

LAWRENCE, J. Introduction to neural networks. California Scientific Software, Nevada City. 1993.

LEE, C. and STERLING, R. Identifying probable failure modes for underground openings using a neural network. *Int. J. Rock Mech. Min. Sci. & Geomech.* Abstr. 29, 1992. pp. 49–67.

MASTER, T. Practical neural network recipes in C++. Academic Press, Inc., Santiago, CA. 1993.

MUNSON, D.E., *et al.* Overtest for simulated defence high-level waste (Room B) : *In situ* data report, SAND 89-2671, Sandia National Laboratories, Albuquerque, New Mexico. 1990.

STERLING, R.L and LEE C.A. A neural network - Expert system hybrid approach for tunnel design. *Proc. of the 33rd U.S. Symp. on Rock Mechanics*, Sandia National Laboratories, Santa Fe, 1992. pp.501–510.

SZEWCZYK, Z.P. and HAJELA, P. Damage detection in structures based on feature-sensitive neural networks. *J. of Computing in Civil Engineering* 8, 1994. pp. 163–178.

THOMAS, A.L. and LA POINTE, P.R. Conductive fracture identification using neural networks. *Proc. of the 35th U.S. Symp. Rock Mechanics,* University of Nevada, Reno, 1995. pp. 627–632.

ZHANG, Q., SONG, J., and NIE, Z. Application of neural network models to rock mechanics and rock engineering. *Int. J. Rock Mech. Min. Sci. & Geomech.* Abstr. 28, 1991. pp. 535–540. ◆